An Efficient Computational Tool for Ramjet Combustor Research

S.P. Vanka[*], J.L. Krazinski[*]
Argonne National Laboratory, Argonne, IL
and
A.S. Nejad[**]
AFWAL/POPT, Wright Patterson Air Force Base, OH

Abstract

A multigrid-based calculation procedure is presented for the efficient solution of the time-averaged equations of a turbulent, elliptic-reacting flow. The equations are solved on a non-orthogonal curvilinear coordinate system. The physical models currently incorporated are a two-equation k-ε turbulence model, a four-step chemical kinetics mechanism, and a Lagrangian particle-tracking procedure applicable for dilute sprays. Demonstration calculations are presented to illustrate the performance of the calculation procedure for a ramjet dump combustor configuration.

Nomenclature

a_p	total area of droplets
A_i	coefficients in the finite-difference equations
$a_1..a_4,$	constants in the reaction rates
$b_1..b_4,$	
$c_1..c_4$	
$C_1..C_4$	constants of geometry transformation
C_p	specific heat of liquid droplets
C_μ	constant in the turbulence model
C_b	boiling constant
C_D	drag coefficient
d_p	diameter of liquid droplet
E1..E4	activation energies for the reaction rates
F	correction factor in reaction rate expression
G	generation of turbulence energy
h	heat transfer coefficient between the gas and the liquid droplets
J	Jacobian of the coordinate transformation
k	turbulence kinetic energy

L	latent heat of evaporation
m_i	species mass fractions
M_i	species molecular weights
m_p	mass of liquid droplet
Nu	Nusselt number
p	pressure
Pr	Prandtl number
r	radius
R	universal gas constant
Re	Reynolds number
S^ϕ	source term
S^m, S^u	sources of mass m and momentum u due to evaporation
t	time
T	gas temperature
T_p	particle temperature
u,v	cartesian velocities
u_p	particle velocity in x direction
U,V	contravariant velocities
V_p	total velocity of particle
$\underline{V}$	total velocity of gas
w	swirl velocity
x,y	cartesian coordinate directions
X_p	particle position
$x_1..x_4$	exponents in the reaction rates
$x_\xi, x_\eta,$ y_ξ, y_η	coordinate transformation derivatives

Greek symbols

α, β, γ	coordinate transformation variables
Γ^ϕ	exchange coefficient
ξ, η	transformed coordinate directions
ϕ	general variable
μ	laminar viscosity
μ_t	turbulent viscosity
λ	fluid thermal conductivity
ρ	fluid density
ρ_p	particle density
ε	rate of dissipation of turbulent energy
ϕ	initial equivalence ratio

Introduction

Integral ramrockets are being considered as propulsion devices for advanced missile systems [1,2]. In these designs, the cruise phase propulsion is achieved by combusting liquid or gaseous fuel in the empty space left by the solid propellant. The combustor configuration is a simple dump with no secondary air injection. The flame holding is usually achieved in the corner recirculation region, and is sometimes aided by imparting swirl to the inlet stream. Liquid fuel is injected into the inlet arm (Fig.1) and vaporized and ignited in the dump. The efficient design of such a propulsion system requires a clear understanding of the complex combustor dynamics and the influence of the various geometric and flow parameters.

A number of complexities are encountered in the dump combustor. Although the ramjet combustor configuration is simpler than that of a gas turbine engine, the fluid mechanics and combustion phenomena are still very complex. The most important aspect is turbulence and its impact on fuel-air mixing and combustion. In the case of liquid fuel injection, additional complexities arise from the breakup, evaporation, and combustion of the liquid film and the droplets. The transport of these droplets with the air stream is also complicated because of the effects of turbulent dispersion. Thus, the ramjet combustor not only provides a challenging design task for the engineer, but it also represents a geometrically simple configuration with significant opportunities for research in turbulent reacting flows.

A large amount of literature exists in turbulent reacting flows [3]. The experimental research has ranged from very fundamental issues such as mixing within the turbulent eddies, to the overall measurement of bulk quantities such as combustion efficiencies and pressure drops. The analytical research has also spanned the range from the simplest form of correlating key parameters, to the ultimate direct simulation of turbulence and turbulent mixing. The simple models are highly economical to use (with practically no computational costs) but cannot always be relied upon. On the other hand, the direct simulation approach is very rigorous; however, because of its excessive computational work, it presently cannot be used for practical flows, and certainly not for industrial design.

This paper deals with the solution of the multidimensional time-averaged steady state Navier-Stokes equations in conjunction with models for turbulence, mixing, chemical kinetics, etc. The solution to the time-averaged equations can represent the multidimensional spatial variations and still be economical enough to be used by industrial designers. Because of its superiority over simpler models, the time-averaged approach has been quite popular in the past decade.

The computational cost for a multidimensional time-averaged fluid flow calculation can be large if the equations are not solved with the optimal solution algorithm. A recent systematic assessment [4,5] of a popularly used methodology [6] revealed that the computational burden of a time-averaged calculation can be quite large (and unaffordable), especially for three-dimensional flows. Therefore, the authors' recent research has been focused on reducing these costs so that design sensitivity analyses and development of the mathematical models can be performed economically. The objective of this paper is to describe this research effort and to demonstrate the performance of the alternative calculation scheme.

The work described here is an extension of previously reported work by the authors [7]. The contributions of this paper are a more robust iterative procedure (especially for swirling flows), incorporation of a four-step reaction scheme, extension to non-orthogonal systems, and the representation of liquid fuel transport. The mathematical models used in this study are those frequently used in the literature.

Equations Solved

The fundamental assumption in the present formulation is that the flow is time-mean steady. The effects of fluctuations of all frequencies (both low and high) are captured through a single, time-invariant model that relates them to the time-mean flow variables. While the universality and scientific rigor of such models is to some extent questionable, their use as an engineering tool is significant. Therefore, research into improving their performance is a worthwhile task.

The governing equations for a time-averaged turbulent reacting flow have been presented in several earlier works [8] and can be expressed in a

general form. For solution on non-orthogonal meshes, it is first necessary to select the velocity components for which the momentum equations are solved. Among the alternatives available, the equations for the Cartesian (x,y) velocities have a simpler formulation. The transport equations with these flow velocities can be written as [9]

$$\partial/\partial\xi \, (\rho U\phi) + \partial/\partial\eta \, (\rho V\phi) = \partial/\partial\xi \, (C_1 \, \partial\phi/\partial\xi +$$
$$C_2 \, \partial\phi/\partial\eta) + \partial/\partial\eta \, (C_3 \, \partial\phi/\partial\eta + C_4 \, \partial\phi/\partial\xi) + S^\phi \tag{1}$$

where (ξ,η) are the coordinates in the curvilinear system and U and V are the contravariant velocity components given by

$$U = y_\eta u - x_\eta v ; \tag{2}$$

$$V = x_\xi v - y_\xi u . \tag{3}$$

u and v are the Cartesian velocities, and x_ξ, y_ξ, x_η, y_η define the local alignments of the coordinate system. S^ϕ is a source term, given in Table I for each equation. C_1, C_2, etc., are given by

$$C_1 = \Gamma^\phi \, \alpha \, / \, J;$$

$$C_2 = C_4 = -\Gamma^\phi \, \beta \, / \, J ;$$

$$C_3 = \Gamma^\phi \, \gamma \, / \, J;$$

$$\alpha = x_\eta{}^2 + y_\eta{}^2 ;$$

$$\beta = x_\xi x_\eta + y_\xi y_\eta ;$$

$$\gamma = x_\xi{}^2 + y_\xi{}^2 ;$$

$$J = x_\xi y_\eta - x_\eta y_\xi . \tag{4}$$

The quantity ϕ represents the Cartesian velocities u and v, the scalars such as the turbulence variables, and the chemical species. The mass continuity equation is obtained by setting ϕ to unity.
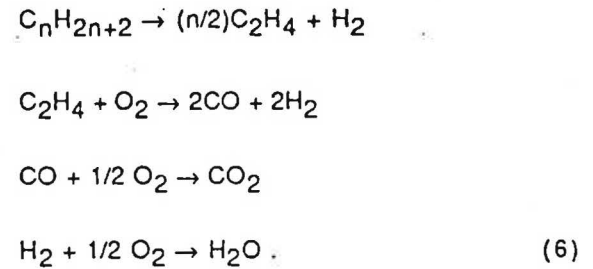
The turbulence model currently used is the k-ε model in which transport equations are solved for the turbulence kinetic energy and its rate of dissipation. The isotropic turbulent viscosity is

calculated from the relation

$$\mu_t = C_\mu \, \rho \, k^2/\varepsilon \tag{5}$$

with $C_\mu = 0.09$. Near the wall, wall functions are used to capture the effects of steep near-wall gradients. The wall function treatment is the same as that originally proposed in ref. 10.

The mixture density is computed from the perfect gas law, and the mixture composition is evaluated through a four-step chemical kinetic scheme. The four-step scheme currently incorporated was proposed by Hautman et al. [11] for a general aliphatic hydrocarbon, assuming it to first reduce to C_2H_4. The four steps in the global kinetics scheme are

$$C_nH_{2n+2} \rightarrow (n/2)C_2H_4 + H_2$$

$$C_2H_4 + O_2 \rightarrow 2CO + 2H_2$$

$$CO + 1/2 \, O_2 \rightarrow CO_2$$

$$H_2 + 1/2 \, O_2 \rightarrow H_2O . \tag{6}$$

The reaction rate expressions are

$$d/dt \, [C_nH_{2n+2}] = -10^{x_1}exp(-E_1/RT)$$
$$[C_nH_{2n+2}]^{a_1} \, [O_2]^{b_1}[C_2H_4]^{c_1}$$
$$mole/cc\text{-}s$$

$$d/dt \, [C_2H_4] = -10^{x_2} \, exp \, (-E_2/RT)[C_2H_4]^{a_2}$$
$$[O_2]^{b_2}[C_nH_{2n+2}]^{c_2} \, mole/cc\text{-}s$$

$$d/dt \, [CO] = \{-10^{x_3} \, exp(-E_3/RT)[CO]^{a_3}[O_2]^b$$
$$[H_2O]^{c_3}\} \, x \, F \, mole/cc\text{-}s$$

$$d/dt \, [H_2] = -10^{x_4} \, exp(-E_4/RT)[H_2]^{a_4}[O_2]^b$$
$$[C_2H_4]^{c_4} \, mole \, /cc\text{-}s \tag{7}$$

where a_1, etc., are given in Table 2.

$$F = 7.93 \, exp(-2.48 \, \Phi)$$

where Φ is the initial equivalence ratio, and F is always less than one.

Integration of (13) gives the droplet diameter as

$$d_p^2 = (d_p^2)_{old} - C_b(1 + 0.23\ Re^{0.5})\Delta t \quad (15)$$

The above set of equations essentially 'closes' the mathematical model. The solution of these equations can only be achieved numerically by either a finite-difference or a finite-element procedure. The following section describes a finite-difference procedure for solving the above equations.

Solution Procedure

Equations similar to those given above have been numerically solved in a number of previous studies of turbulent reacting flows [3]. The numerical procedure commonly employed is based on the SIMPLE algorithm [6] incorporated in variants of the TEACH computer program. A common experience with such a procedure has been that the computer times are large and the convergence is slow, especially when fine grids are considered.

The solution procedure presented here is based on the block implicit multigrid procedure originally presented in ref. 19. In recent studies [7], this procedure was observed to be rapidly convergent in a number of problems and to produce significant reductions in required computational times. Therefore, in this study, it has been extended to include other features that characterize a practical reacting flow.

Finite-differencing

The discretization of the transport equations closely follows the earlier scheme proposed by Spalding [20] in which the convective and diffusive terms are discretized through a hybrid differencing procedure. This procedure has been used in several of the earlier works and remains the preferred method from a stability viewpoint, although it is accurate only to the first order. The source terms are integrated by calculating an average value in a finite volume. Because this approach is well known, it is not detailed here. The outcome of the differencing scheme is a set of- linear coupled equations of the form

$$A_p\ \phi_P = \Sigma\ A_i\ \phi_i + \underline{S}^{\phi} \quad\quad (16)$$

where the A's are the finite difference coefficients.

One difference between the present scheme and previous ones lies in the retention of the primitive continuity equation rather than converting it to a pressure or pressure correction equation. The primitive continuity equation has the merit of tight coupling between velocities and pressures and can converge faster than a decoupled procedure.

Solution of Momentum and Continuity Equations

The finite-differenced momentum and continuity equations are solved by a coupled multigrid technique as described in ref. 7. The velocities and pressures are simultaneously updated without the use of a pressure or pressure correction equation. The tight coupling between the momentum and continuity equations provides rapid convergence of the iterative procedure. Another important aspect of the present procedure is the use of the multigrid technique to accelerate the rate of convergence on fine grids. In the multigrid procedure, the low-frequency errors in the solution are resolved on coarser grids, and corresponding corrections are applied to the fine grid values. The coarse and fine grids are continuously cycled in an adaptive manner.

The relaxation procedure (iteration scheme) used here differs from that presented in ref. 7 in the manner by which the coefficients are updated. By contrast with the earlier procedure, in the present scheme the coefficients in the finite-difference equations are all evaluated with the old iterate values and stored. The coupled momentum and continuity equations are then solved by repeated (typically three) sweeps of a symmetrically coupled Gauss-Seidel (SCGS) operator. In the SCGS scheme, the velocities on all four cell faces and the pressure are simultaneously corrected on the basis of the residuals in the momentum and continuity equations. The corrected velocity and pressure fields are subsequently restricted to coarser grids, and the low-frequency components in the residual are resolved. One solution step of the momentum and continuity equations consists of one iteration on the locally finest grid and a few sub-iterations on the coarse grids. The coarse-grid cycling is performed until the residual is decreased to a fraction (0.4) of the fine-grid value.

Solution of the Chemical Kinetics Equations

The equations describing the formation of the individual species are locally tightly coupled

through the source and sink terms. The resolution of these local source terms is much more important than the convective and diffusive transport due to the flow field. To resolve this close coupling between the species, it is necessary to iterate between the species equations, updating the respective source terms.

In the present solution framework, the chemical kinetic equations are solved by a single-grid technique. The calculation sequence for one iteration on the scalar equations is as follows.

    a. Select a scalar.

    b. Assemble convection and diffusion coefficients.

    c. Calculate source terms.

    d. Perform one Gauss-Seidel sweep of the domain.

    e. Repeat (a) - (d) for all scalars.

    f. Repeat (a) - (e), typically 5 times.

The finite-difference coefficients need not be updated if the Prandtl/Schmidt numbers for the species are assumed to be equal; otherwise, they need to be re-evaluated in step (b). The updated values of the species are used in the evaluation of a new density field.

Calculation of Particle Trajectories

The trajectories of the individual groups of droplets are calculated by a Lagrangian method. For each group, the initial velocities, position, droplet diameter, temperature, and number density are specified. These values (except number density) are then updated by following the trajectory of the particle. If the particles collide with the wall boundaries, perfect reflection is assumed. The trajectory is terminated at an outflow location. The sources of fuel, enthalpy, and momentum are calculated for each finite volume by summing the contributions from all groups of droplets. Thus,

$$(S^m)_{i,j} = \Sigma_k \{(\rho_p \underline{V}_p)_{in} - (\rho_p \underline{V}_p)_{out}\}$$

$$(S^u)_{i,j} = \Sigma_k \{(\rho_p u_p^2)_{in} - (\rho_p u_p^2)_{out}\} \quad (17)$$

etc., k = 1, number of particle groups. Typically, 5-10 particle groups are used in the calculation.

The sources for the species are generated by evaporation of the liquid droplets. These sources are then used in the respective transport equations for the calculation of the distributions of the species.

The particle trajectory calculations are not of the finite-difference type. Thus they do not employ the multigrid framework. However, the particle trajectories are calculated on the coarser grids in the full multigrid (FMG) cycle. Thus, a good estimate of the density field is generated prior to the solution on any fine grid.

Demonstration Calculations

The complete development and validation of the various submodels for chemical kinetics, spray transport, and turbulence requires a considerable amount of analytical and experimental effort. The success of such an effort greatly depends on the numerical scheme employed for the solution of the equations. In this section, results of some demonstration calculations are provided to illustrate the convergence of the present algorithm. For each test case, plots of the rate of convergence are shown, and the benefit of multigrid cycling is demonstrated. Some comparisons with actual experimental data were presented earlier [21]. However, significant further development and validation is necessary before the models and the associated computer program can be used for regular engineering design.

Isothermal Flow in a Sloping-Wall Combustor

Figure 2 shows a dump combustor with the top wall sloping at an arbitrary angle and with a nozzle at the exit. Depending on the slope of the outer wall, a recirculation zone formed at the corner of the dump can be used for stabilizing the combustion process. The pressure drop and combustion characteristics can be optimized by varying the slope and the length of the combustor.

Demonstration calculations have been made for an inlet velocity of 20 m/s and for different angles of the outer wall. The dimensions of the configuration are shown in Fig. 2. Calculations have been made for three finite-difference grids of increasing fineness. The grids contained 10 x 5, 20 x 10, and

40 x 20 cells in the x and radial directions, respectively. The coordinate lines in the radial direction were aligned to the outer wall, whereas the axial lines were of constant x values. The coarsest grid in the calculations contained 10 x 5 cells in the x and r directions. The tolerance criterion on the momentum residual was set to 1.0e-3. Figure 3 shows the rates of convergence and the calculated streamlines for an outer wall slope of 45 degrees. The residual plotted is of the u-momentum equation. The total number of work units, including the coarse grid work, is approximately equal to twice the number of iterations shown in the plot.

The three grids in Fig. 3 converge at nearly the same rate, and convergence is achieved in about 20 fine-grid iterations. The streamlines and the calculated distributions of other variables behave according to expectations, but quantitative comparison with experimental data is necessary.

The influence of the outer-wall slope on the rate of convergence and the streamline patterns is shown in Figs. 4 and 5 for two other angles. The convergence for smaller angles is slightly better than that of the previous case, presumably because of the lack of flow recirculation in the latter two cases. The present procedure of solving for the Cartesian velocities has limitations on the inclination of the grid lines, and the convergence is empirically observed to become difficult after about 45 degrees of inclination [7]. However, this limitation can be removed by solving either for the covariant velocities or for two components on each face [9].

Influence of Swirl

In many combustors, swirl is imparted to the air stream to improve the mixing of fuel and air. Swirl can also be used to stabilize the flame by the creation of a central recirculation zone (CTRZ). However, swirl can have the adverse effect of eliminating the corner recirculation zone that is actively relied upon for flame holding.

The dynamics of swirling flows are quite complex. Recent studies [21] in a dump combustor have revealed unsteady flow fields that are difficult to predict through the solution of the time-averaged Navier-Stokes equations. Swirl is known to cause precessing vortex cores and complex turbulence behavior. Despite these complexities, the predictions with time-averaged equations and a

two-equation model can guide the design process in the correct qualitative direction. The numerical solution of the equations of a swirling flow is also difficult because of the presence of body forces and strong radial pressure gradients. Furthermore, the prescription of the conditions at the inlet to the solution domain is difficult because of the uncertainty of the turbulence characteristics at the swirler exit.

The influence of inlet swirl on the rate of convergence is shown in Figs. 6 to 8. The inclusion of swirl somewhat slows down the rate of convergence, because of the nonlinear coupling between the swirl equation and the other momentum and continuity equations. In the current calculations, a constant-angle vane swirler with a hub of 1-inch diameter is assumed to provide the swirl. A plug swirl velocity distribution is currently used, but there is no restriction on the profile that can be prescribed. For the two swirl velocity ratios calculated here (w/u = 1.0 and 1.5), a central recirculation zone was observed.

Premixed Combustion in a Sudden Expansion

The next case considered is the premixed combustion of a stoichiometric mixture of propane and air with the composition given in ref. 11. The four-step reaction is considered with rate constants given by Hautman et al. [11]. The inlet temperature of the mixture is taken to be 1130 K. The density is updated after each solution of the chemical kinetic equations, and an under-relaxation factor of 0.6 is used on the density to procure stable convergence.

Figure 9 shows the convergence plot for the reacting flow. The convergence criterion is the same as before and is based on the residual in the x-momentum equation. The chemical kinetic equations are solved by a fixed number of sweeps (10), and their successive changes at convergence are observed to decrease below 1.0e-5. The convergence of the chemical kinetic equations influences the overall convergence through changes in the density.

Calculation with Sprays

The demonstration calculations with the inclusion of liquid droplets have been made only for the isothermal case. Here the spray has no effect on the rate of convergence, as the interaction of the

spray with the flow field through evaporation and combustion of the fuel has not been exercised. Spray calculations with combustion will be pursued in future studies.

Summary

A calculation procedure based on the block-implicit, multigrid solution of the momentum and continuity equations has been extended to include non-orthogonal coordinates, multistep chemical kinetics, and liquid droplet combustion. Because of the strong influence of the source terms in the chemical kinetic equations, a single-grid procedure with repeated update of the source terms is currently used. In the non-orthogonal system, equations are solved for the Cartesian velocities. The droplet transport is incorporated by a Lagrangian particle tracking procedure that accounts for the droplet drag. The evaporation of the droplets is modeled through empirical relations characterizing single drops.

The intent of this paper has been to demonstrate the feasibility of performing efficient calculations of time-averaged fluid flows characteristic of subsonic ramjet combustors. The present solution methodology holds promise for efficiently developing and validating mathematical models for turbulent and reacting flows.

References

1. F.F. Webster, "Liquid Fueled Integral Rocket Ramjet Technology, Review," AIAA-78-1108, AIAA/SAE 14th Joint Propulsion Conference, Las Vegas, NV, 1978.

2. R.R. Craig, J.D. Drewery, and F.D. Stull, "Coaxial Dump Combustor Investigations," AIAA-78-1107, AIAA/SAE 14th Joint Propulsion Conference, Las Vegas, NV, 1978.

3. R.M.C. So, J.H. Whitelaw, and H.C. Mongia, (ed) "Calculations of Turbulent Reactive Flows," Proceedings of the ASME Winter Annual Meeting, 1986.

4. R. Srinivasan, et al., "Aerothermal Modeling Program, Phase-1, Final Report," NASA-CR-168243, Nov. 1983.

5. G.J. Sturgess, "Aerothermal Modeling Program, Phase-1, Final Report," NASA-CR-168202, July 1983.

6. S.V. Patankar and D.B. Spalding, "A Calculation Procedure for Heat, Mass, and Momentum Transfer in Three-Dimensional Parabolic Flows," Intl. J. Heat and Mass Transfer, Vol. 15, p. 1787-1806, 1972.

7. S.P. Vanka, "Block Implicit Multigrid Calculation of Fluid Flows - Recent Results," AIAA-87-0059, 25th Aerospace Sciences Meeting, Reno, NV, 1987.

8. W.P. Jones and J.H. Whitelaw, "Calculation Methods for Reacting Turbulent Flows: A Review," Combustion and Flame, Vol. 48, p. 1-26, 1982.

9. C.R. Maliska and G.D. Raithby, "A Method for Computing Three-Dimensional Flows Using Non-Orthogonal Boundary-Fitted Coordinates," International Journal for Numerical Methods in Fluids, Vol. 4, p. 519-537, 1984.

10. B.E. Launder and D.B. Spalding, "The Numerical Computation of Turbulent Flows," Computer Methods in Applied Mechanics and Engineering, Vol. 3, p. 269-289, 1974.

11. D.J. Hautman, et al., " A Multiple-step Overall Kinetic Mechanism for the Oxidation of Hydrocarbons," Combustion Science and Technology, Vol. 25, p. 219-235, 1981.

12. D.B. Spalding, "Mathematical Models of Turbulent Flames, A Review," Combustion Science and Technology, Vol. 13, p.13, 1976.

13. C.T. Crowe, " Review - Numerical Models for Dilute Gas-Particle Flows," Journal of Fluids Engineering," Vol. 14, No. 3, p. 297-303, 1982.

14. J.S. Shuen, et al., "Structure of Particle Laden Jets, Measurements and Predictions," AIAA Journal, Vol. 23, No. 3, p. 396-404, 1985.

15. G.M. Faeth, "Evaporation and Combustion of Sprays," Progress in Energy and Combustion Science, Vol. 9, p. 1-76, 1983.

16. C.K. Law, "Recent Advances in Droplet Vaporization and Combustion," Progress in Energy and Combustion Science, Vol. 8, p. 171-201, 1982.

17. W.A. Sirignano, " Fuel Droplet Vaporization and Spray Combustion Theory, " Progress in Energy and Combustion Science, Vol. 9, p. 291-322, 1983.

18. Y. El-Banhawy and J.H. Whitelaw, "Calculation of the Flow Properties of a Confined Kerosene Spray Flame," AIAA Journal, Vol. 18, No. 12, p. 1503-1510, 1980.

19. S.P. Vanka, "Block-Implicit Multigrid Solution of Navier-Stokes Equations in Primitive Variables," J. Computational Physics, Vol. 65, p. 138-158, 1986.

20. D.B. Spalding, "A Novel Finite-Difference Formulation for Differential Expressions Involving Both First and Second Derivatives," Intl. J. Numerical Methods in Engineering, Vol. 4, p. 551-559, 1972.
21. M.A. Samimy, et al., "Isothermal Swirling Flow in a Dump Combustor," AIAA-87-1352, 19th Fluid Dynamics, Plasma Dynamics and Lasers Conference, Honolulu, Hawaii, 1987.

Table 1. Source Terms for the Dependent Variables

Variable	Source term
u	$y_\eta\, \partial p/\partial \xi - y_\xi\, \partial p/\partial \eta + (\, y_\eta\, \Gamma_\xi - y_\xi\, \Gamma_\eta\,)\, (\, y_\eta\, u_\xi - y_\xi\, u_\eta\,)\, /\, J +$ $(\, y_\eta\, v_\xi - y_\xi\, v_\eta\,)\, (\, x_\xi\, \Gamma_\eta - x_\eta\, \Gamma_\xi\,)\, /\, J$
v	$x_\xi\, \partial p/\partial \eta - x_\eta\, \partial p/\partial \xi + \rho\, w^2\, /\, r + (\, x_\xi\, u_\eta - x_\eta\, u_\xi\,)\, (\, y_\eta\, \Gamma_\xi - y_\xi\, \Gamma_\eta\,)\, /\, J +$ $(\, x_\xi\, v_\eta - x_\eta\, v_\xi\,)\, (x_\xi\, \Gamma_\eta - x_\eta\, \Gamma_\xi\,)\, /\, J$
w	$-\rho\, v\, w\, /\, r - \Gamma\, w\, /\, r^2 - w\, (\, x_\xi\, \Gamma_\eta - x_\eta\, \Gamma_\xi\,)\, /\, J\, /\, r$
k	$G - \rho\, \varepsilon$ $G = \mu_t\, [\, \{2.0\, \{(y_\eta\, u_\xi - y_\xi\, u_\eta)^2 + (x_\xi\, v_\eta - x_\eta\, v_\xi)^2\} +$ $(y_\eta\, v_\xi - y_\xi\, v_\eta + x_\xi\, u_\eta - x_\eta\, u_\xi)^2 + (y_\eta\, w_\xi - y_\xi\, w_\eta)^2 +$ $(x_\xi\, w_\eta - x_\eta\, w_\xi\,)^2\}\, /\, J^2 - (w/r)^2 + 2.0\, v^2\, /\, r^2\,]$
ε	$1.47\, G\varepsilon/k - 1.92\, \rho\, \varepsilon^2/k$
m_{fu}	$\max(\, R_{ARR}, R_{EBU}\,);\ R_{ARR}$ as per Equation (7) of text. $R_{EBU} = -CR\, m_{fu}\, \rho\varepsilon\, /\, k\ ;\ CR = 3.0$
m_{CH}	$\max(\, R_{ARR}, R_{EBU}\,);\ R_{ARR}$ as per Equation (7) of text. $R_{EBU} = -CR\, \min(m_{CH}, m_{ox} \cdot M_{CH}\, /\, M_{ox})\ \rho\,\varepsilon\, /\, k$
m_{CO}	$\max(\, R_{ARR}, R_{EBU}\,);\ R_{ARR}$ as per Equation (7) of text. $R_{EBU} = -CR\, \min(m_{CO}, m_{ox} \cdot 2.0 \cdot M_{CO}\, /\, M_{ox})\ \rho\,\varepsilon\, /\, k$
m_{H2}	$\max(\, R_{ARR}, R_{EBU}\,);\ R_{ARR}$ as per Equation (7) of text. $R_{EBU} = -CR\, \min(m_{H2}, m_{ox} \cdot 2.0 \cdot M_{H2}\, /\, M_{ox})\ \rho\,\varepsilon\, /\, k$

Table 2. Reaction Rate Constants

Reaction	x	E	a	b	c
1	17.32	49600	0.5	1.07	0.40
2	14.70	50000	0.9	1.18	-0.37
3	14.60	40000	1.0	0.25	0.50
4	13.52	41000	0.85	1.42	-0.56

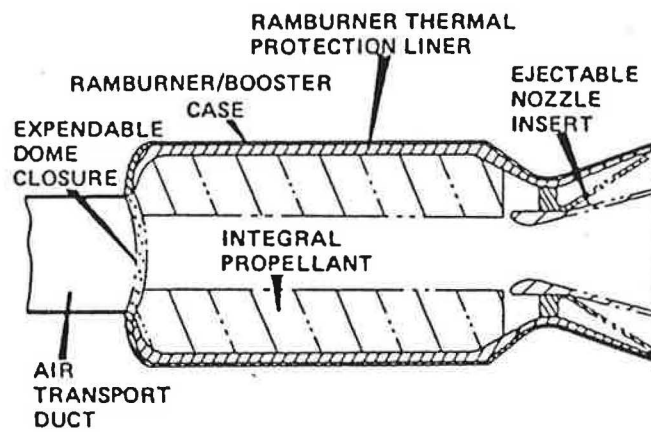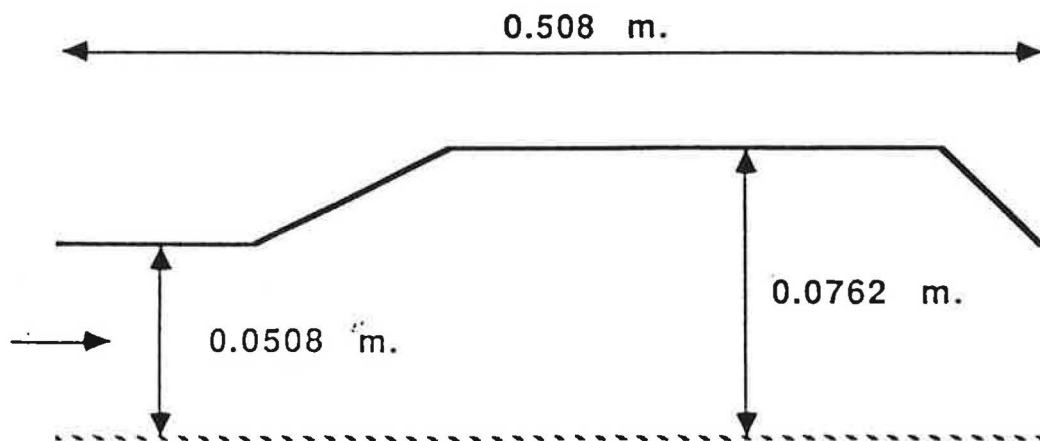Fig. 1. Integral Ramjet/Rocket Concept [1].
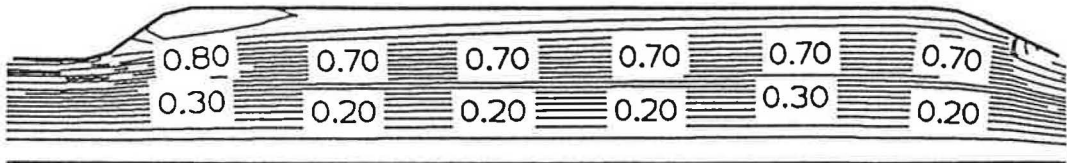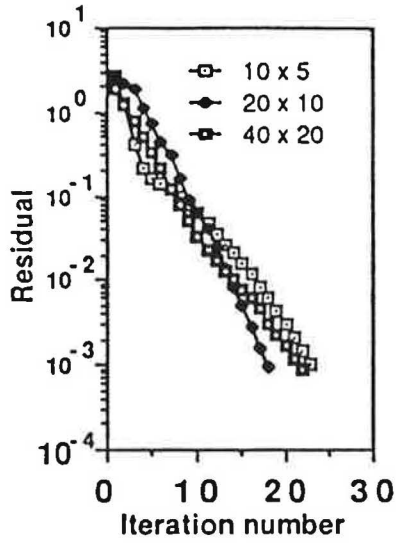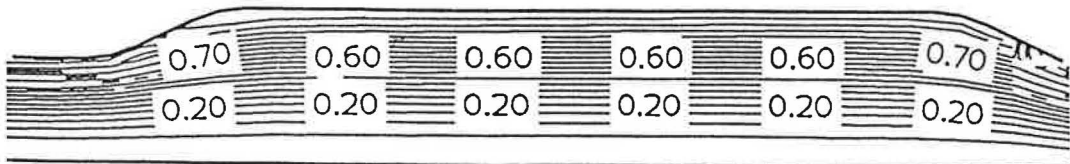

Fig. 2. Geometric configuration.

Fig. 3. Rate of convergence and calculated streamlines,
outer-wall angle = 45 deg.
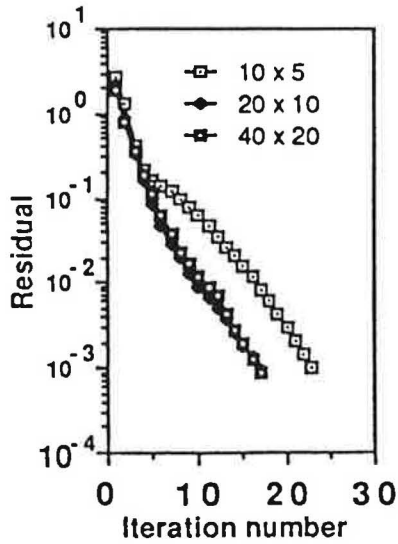
Fig. 4. Rate of convergence and calculated streamlines,
outer-wall angle = 30 deg.
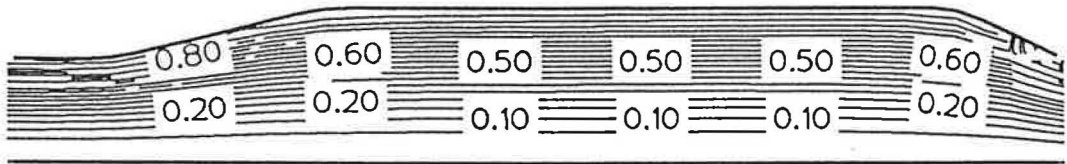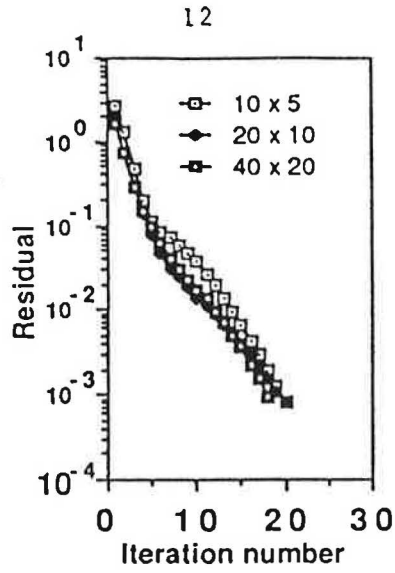
Fig. 5. Rate of convergence and calculated streamlines,
outer-wall angle = 15 deg.
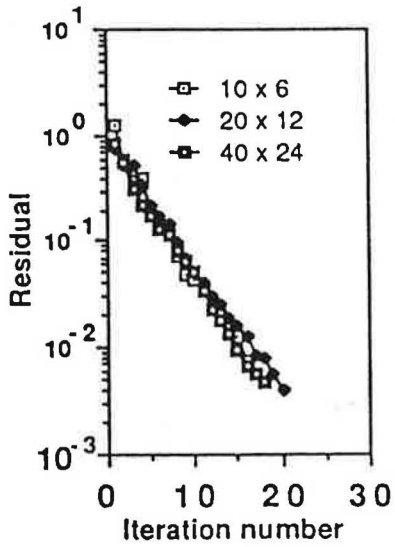
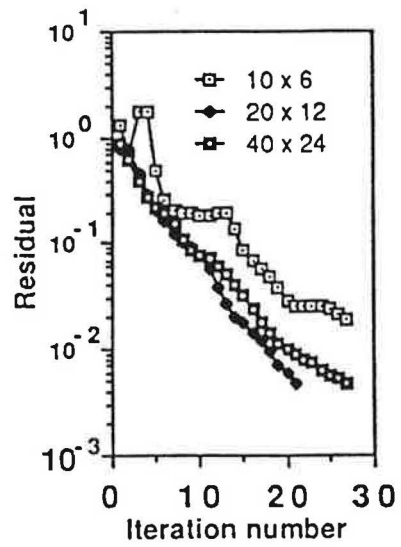Fig. 6. Rate of convergence for turbulent flow in a
sudden expansion, w = 0.

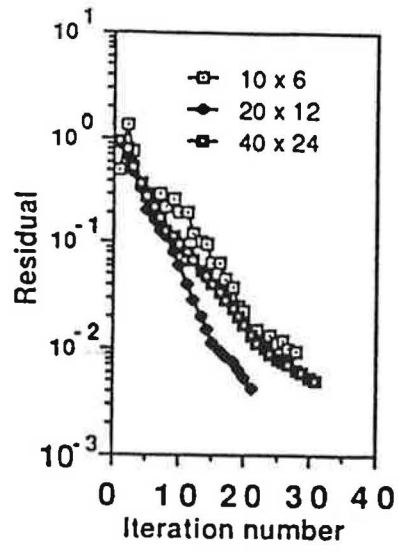Fig. 7. Rate of convergence for turbulent swirling flow
in a sudden expansion, w = u.

Fig. 8. Rate of convergence for turbulent swirling flow
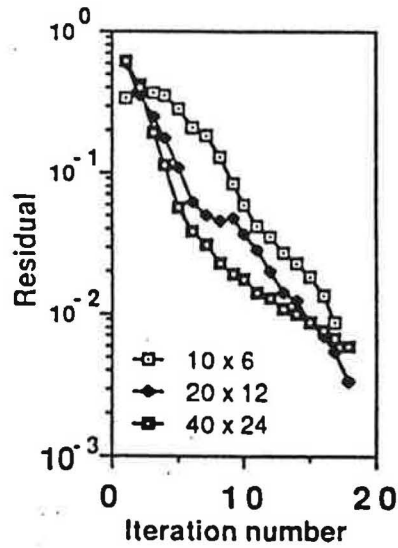in a sudden expansion, w = 1.5 u.

Fig. 9. Rate of convergence for turbulent reacting flow
in a sudden expansion.

AIAA'88

AIAA-88-0060

An Efficient Computational Tool for Ramjet Combustor Research

S. P. Vanka, J. L. Krazinski,
Argonne National Laboratory, Argonne, IL
and
A. S. Nejad,
AFWAL/POPT, Wright Patterson Air
Force Base, OH

AIAA 26th Aerospace Sciences Meeting
January 11-14, 1988, Reno, Nevada.